DOI: 10.1002/ejoc.200601074

Electron-Density Determination of Electrophilic Building Blocks as Model Compounds for Protease Inhibitors

Simon Grabowsky,[a] Thomas Pfeuffer,[b] Lilianna Chęcińska,[a] Manuela Weber,[a] Wolfgang Morgenroth,[c–e] Peter Luger,[a] and Tanja Schirmeister*[b]

Keywords: Aziridine / Charge density / Electron density / Nucleophile / Protease

Three types of synthesised compounds, the aziridine **1**, the epoxide **2** and the acceptor-substituted olefin **3**, were chosen as model compounds for electrophilic building blocks, which can covalently block the nucleophilic amino acids of the active sites of proteases (Cys in cysteine proteases or Asp in aspartate proteases). In order to rationally design optimised inhibitors and to understand the differences in inhibition properties of the scrutinised building blocks their structural and electronic properties were studied by ultra-high resolution X-ray diffraction and ab initio calculations to yield the experimental electron-density distribution. It could be shown that the carbon atom C1 of the three-membered heterocycle is the preferred electrophilic centre for attack of the nucleophiles, which is consistent with the results of corresponding chemical experiments with sulfur and oxygen nucleophiles.

(© Wiley-VCH Verlag GmbH & Co. KGaA, 69451 Weinheim, Germany, 2007)

Introduction

Most biological processes as well as the pharmacological action of most drugs are initiated by a preliminary step in which two molecular species, e.g. a macromolecular target protein and a low-molecular weight ligand, recognise each other and form a complex. Steric as well as electrostatic properties of the two species play dominant roles in these recognition processes.

Ultra-high resolution X-ray diffraction experiments at low temperature cannot only be used to determine atomic connectivity and conformation of compounds, but also to analyse electron-density distribution.[1,2] Bond topological and atomic properties are quantitatively accessible from the three-dimensional distribution of the electron density by application of Bader's QTAIM-theory (QTAIM = Quantum Theory of Atoms in Molecules).[3]

Additionally, the crystallographic experiment yields information on the nature of intermolecular interactions, including charge transfer in co-crystals with more than one molecule. Since molecules are found to have different dipole moments in different crystalline environments due to polarisation effects of the crystal field, an advantage of the experimental electrostatic potential over the potential from isolated molecule calculations is that effects arising from the crystal packing are accounted for. Due to the nature of the molecular interactions these effects will generally cause the molecules to pack in a characteristic way, i.e. the molecules will pack in a key-lock arrangement in which regions of charge concentration face electron-deficient regions in adjacent molecules in the crystal, and in which hydrogen-bond donors will face hydrogen-bond acceptors.[4] Thus, the X-ray charge density contains quantitative information on the electrostatic interactions and the hydrogen bonding network between molecules. These influences can be assumed to be quite often similar to the influence of a protein environment, since the interactions within the crystals are based on the same types of effects as the ligand-target-interactions (steric, electrostatic, hydrogen bonding, van der Waals effects) and are expected to be comparable in size. Due to these similarities the polarisation of the ligand within the crystal and the protein environment should also be comparable. As a consequence the properties extracted from ultra-high resolution X-ray data of a ligand are often much better suited to simulate physiological conditions than those calculated for an isolated ligand molecule. This has already been shown for the antithrombotic drug terbogrel,[5] the neurotransmitter taurine,[6] and the *anti*-leukemia drug busulfan.[7] For the latter the topological electron-density descriptors were also used to explain its chemical reactivity, namely its alkylating property.

[a] Freie Universität Berlin, Institut für Chemie und Biochemie/Kristallographie,
Fabeckstr. 36a, 14195 Berlin, Germany
[b] University of Würzburg, Institute for Pharmacy and Food Chemistry,
Am Hubland, 97074 Würzburg, Germany
Fax: +49-9318885494
E-mail: schirmei@pzlc.uni-wuerzburg.de
[c] Institut für Anorganische Chemie, Georg-August-Universität, Tammannstraße 4, 37077 Göttingen, Germany
[d] Department of Chemistry, Aarhus University, Langelandsgade 140, 8000 Aarhus C, Denmark
[e] c/o DESY/HASYLAB, Notkestraße 85, 22603 Hamburg, Germany

Supporting information for this article is available on the WWW under http://www.eurjoc.org or from the author.

 © 2007 Wiley-VCH Verlag GmbH & Co. KGaA, Weinheim

Besides information on reversible target ligand binding processes which are mainly based on electrostatic interactions, high resolution X-ray data can also give valuable insight into irreversible binding mechanisms which are always based on the forming of a covalent bond between ligand and target. Since the first stage of a chemical reaction, i.e. the alignment of the involved molecules, is determined by their electrostatic potentials the measured electron density of the ligand allows estimates where the chemical bond is formed if the nature of the attacking centre of the active site is known (e.g. nucleophilic attack by a negatively charged centre of the active site of an enzyme). Even detailed information about the reactivity, the reaction mechanisms, and the reaction rates may be possible. Here, the proof of principle was given already by the electron-density analysis of busulfan,[7] and penicillin derivatives.[8]

Our efforts direct to the development of cysteine[9] and aspartic protease inhibitors[10] consisting of an electrophilic building block (aziridine,[11,12,15] epoxide[13,14] or acceptor-substituted olefin[15,16]) which can covalently block the nucleophilic amino acids of the enzymes' active sites (Cys in cysteine proteases or Asp in aspartate proteases). In order to rationally design optimised inhibitors and to understand the differences in inhibition properties of the scrutinised building blocks we synthesised and crystallised three model compounds **1**, **2**, and **3**. These compounds contain the same substituents (two methyl ester groups at C2, *p*-nitrophenyl moiety at C1), but differ in the type of electrophile: aziridine **1**, epoxide **2**, acceptor-substituted olefin **3**. The nitro-substituted compounds were chosen due to their enhanced crystallisation properties in comparison to the derivatives lacking the nitro group. The electron densities of the compounds were derived from both, high-resolution X-ray diffraction experiments at ultra-low temperature (for **1**), and ab initio calculations (for **1**–**3**). The results of the experimentally and theoretically obtained electronic properties as well as the electronic properties of the three different types of electrophiles are compared. In addition, these data are compared with the reactions of aziridine **1** with sulfur, and oxygen nucleophiles, as model reactions for the inhibition of cysteine and aspartic proteases, respectively.

Results and Discussion

Geometric Results

The experimental conformation of the examined aziridine **1** including thermal ellipsoids at 9 K and the atom numbering scheme chosen is shown in Figure 1. A summary of selected geometric data for both molecules of the asymmetric unit (Table 1) shows that the average difference of bond lengths and angles is 0.003 Å and 0.7°, respectively. Moreover, topological properties do not differ significantly, so that the following discussion is based on the quantitative results obtained from molecule **1** if not otherwise stated.

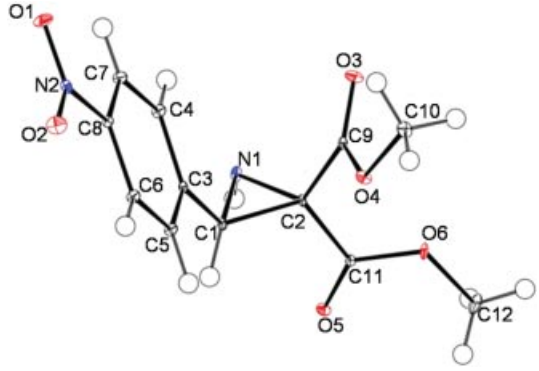

Figure 1. ORTEP[17] representation with displacement ellipsoids at 9 K (50% probability) of aziridine **1** with atom numbering scheme. Hydrogen atoms represented by small spheres of arbitrary radii.

Due to the highly strained three-membered aziridine ring the intra-ring angles are far apart from the normal tetrahedral angles as Table 1 shows. Inside the ring the angles are about 60°, outside between 115.5 and 118° without differences whether an aryl group is connected to the carbon atom (C3–C1–N1 116.5°) or an ester group (e.g. C11–C2–N1 115.8°). But considering the bond lengths there is a small difference between the bond to the aryl group (C1–C3 1.49 Å) or to the ester groups (C2–C9, C2–C11 1.51 Å). The bonds and angles inside the aziridine ring can be compared to the corresponding values of the unsubstituted (free) aziridine by a study from Mitzel et al. at 145 K.[18]

Table 1. Bond lengths [Å], angles [°] and torsion angles [°] for the aziridine ring of aziridine **1** and its direct environment (first–second line: molecule **1**–**2** of the asymmetric unit; third line: free aziridine, taken from ref.[18]).

C1–N1	1.4558(4)	C1–N1–C2	62.45(2)	C4–C3–C1–N1	3.8(1)
	1.4609(7)		62.07(3)		21.5(1)
	1.4640(18)		59.83(9)	N1–C2–C9–O4	141.0(1)
C2–N1	1.4573(4)	N1–C1–C2	58.83(2)		140.6(1)
	1.4621(7)		59.04(3)	N1–C2–C11–O6	143.6(1)
	1.4628(18)		60.05(9)		152.5(1)
C1–C2	1.5100(4)	N1–C2–C1	58.81(3)		
	1.5076(6)		58.89(3)		
	1.4600(20)		60.12(9)		
C1–C3	1.4907(5)	C3–C1–N1	115.71(3)		
	1.4920(7)		117.19(4)		
C2–C9	1.5059(4)	C9–C2–N1	118.12(3)		
	1.5096(6)		116.46(3)		
C2–C11	1.5051(4)	C11–C2–N1	115.55(3)		
	1.5022(6)		116.14(3)		

 © 2007 Wiley-VCH Verlag GmbH & Co. KGaA, Weinheim

These values are likewise given in Table 1. In the free aziridine the three bond lengths and the three angles are almost equal within the error margins (1.46 Å and 60.0°). In the substituted aziridine the C1–C2 distance increases by 0.05 Å, the C–N distances decrease by about 0.01 Å, so that one side of the triangle is lengthened and the angle opposite to this side has to expand. This effect is evident here: The angle C1–N1–C2 increases from 59.8 to 62.2° and the other angles decrease from 60.1 to 58.9°. The three torsion angles listed in Table 1 are the most representative for the conformation of the molecule because the aryl group including the nitro group being in resonance with the phenyl ring is very planar and rigid in its conformation. The two chains consisting of an ester and a methyl group are rigid, too. Therefore significant torsions should only occur at connections of the substituents to the aziridine ring. Comparing the conformation of the molecule shown in Figure 1 to that of the second molecule in the asymmetric unit and to the optimised geometry one can state that the overall conformation is very rigid and that the experimental geometry is very near the gas phase geometry with minimum molecular energy. The energy of a single-point calculation at the experimental geometry differs only by 3.7 kcal mol^{-1} from the energy of a geometry optimisation. All the geometrical parameters only differ slightly when going from one molecule of the asymmetric unit to the other or to the optimised geometry. Due to the molecule's small structural changes when changing the environment, all the results derived from the experimental and theoretical electron-density distribution should be a good estimate for the molecule's properties in biological systems, too.

Figure 2 shows an extract from the crystal packing. The aziridine compound tends to build up layers. The molecules inside a layer are held together by electrostatic contacts like the C11–O3A contact (see below) whereas the molecules in two different layers are connected by hydrogen bonds. In one layer the nitrogen atom of the aziridine ring alternates with the oxygen atom of a carbonyl group. Thus, the stabilising hydrogen bonds N1A–H1NA···O5A and N1–H1N···N1A must alternate, too, forming an angle of about 90° between each other. Table 2 shows the geometric parameters of these two hydrogen bonds and several C–H···acceptor contacts. These contacts are not just found by distance criteria but are known in the literature[21] to be weak interactions that help stabilising the crystal. They have been shown to be important in several drug binding processes.[21] For the present structure they will be discussed later in this article with the aid of Hirshfeld surfaces and topological analyses.

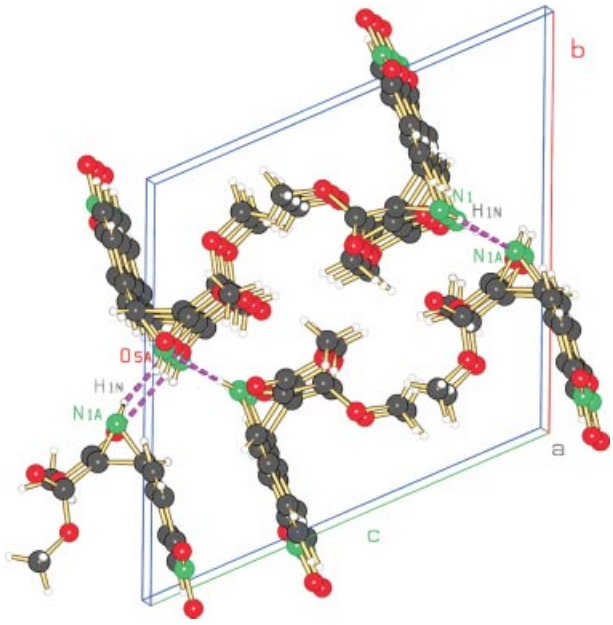

Figure 2. Crystal packing and hydrogen bonding network (SCHAKAL[20] representation).

Electron Deformation and Laplacian Density

Figure 3 shows the experimental negative Laplacian distribution in the plane of the aryl group of aziridine **1**. It is obvious that all bonds are open-shell interactions, i.e. covalent bonds, as the typical saddle shape distributions in the bond regions indicate. Since Figure 3 shows all expected features in the bonding and non-bonding regions it can be concluded that the density distribution was adequately modelled by the multipole formalism.

Table 2. Hydrogen bond geometries, topological parameters and energies.

donor–H···acceptor	r(H···acc) /Å	r(don···acc) /Å	a(don–H···acc) /°	ρ /e Å^{-3}	$\nabla^2\rho$ /e Å^{-5}	E_{HB}[j] /kJ mol^{-1} a_0^{-3}
N1A[a]–H1NA···O5A[c]	2.232(9)	3.113(9)	145.1(1)	0.088(9)	1.6(1)	9.54
N1–H1N···N1A	2.220(9)	3.113(9)	168.8(1)	0.092(9)	1.6(1)	9.46
C5–H5···O1[d]	2.432(10)	3.437(10)	153.8(1)	0.043(11)	0.8(1)	4.79
C5A–H5A···O1A[e]	2.441(10)	3.470(10)	158.4(1)	0.040(11)	0.8(1)	4.85
C6–H6···O4[f]	2.335(9)	3.244(9)	140.4(1)	0.067(10)	1.1(1)	6.43
C7–H7···O5[g]	2.341(9)	3.148(9)	130.0(1)	0.074(13)	1.1(1)	6.30
C7A–H7A···O5A[h]	2.458(9)	3.224(9)	126.7(1)	0.065(12)	0.9(1)	5.07
C10–H10B···O6A[i]	2.415(10)	3.428(10)	158.3(1)	0.057(11)	1.0(1)	5.92
C12A–H12D[b]···N1[d]	2.387(10)	3.383(10)	155.1(1)	0.078(9)	1.2(1)	6.92

[a] Labels A refer to the second molecule of the asymmetric unit. [b] Atom H12D belongs to the second molecule of the asymmetric unit. Symmetry operations. [c] $-x$, $1-y$, $1-z$ (A). [d] $-1+x$, y, z. [e] $-1+x$, y, z (A). [f] $2-x$, $2-y$, $1-z$. [g] $1+x$, y, z. [h] $1+x$, y, z (A). [i] $1-x$, $1-y$, $1-z$ (A). [j] Hydrogen bond energy calculated according to Espinosa et al.[19]

 © 2007 Wiley-VCH Verlag GmbH & Co. KGaA, Weinheim

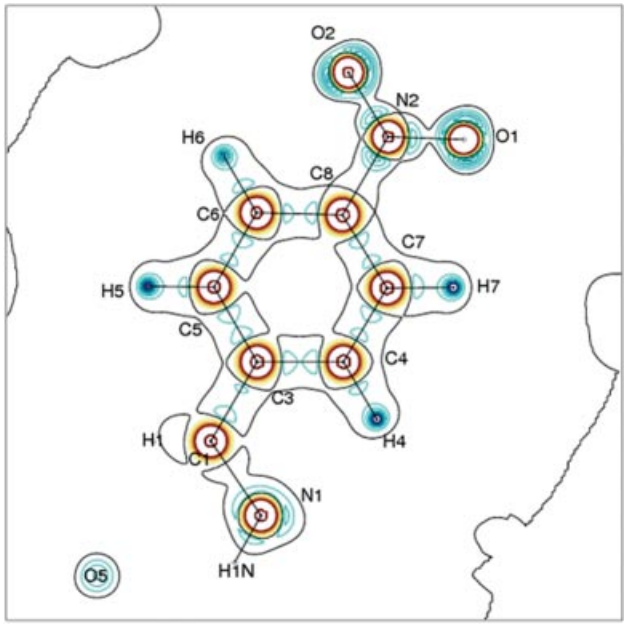

Figure 3. Experimental negative Laplacian distribution in the plane of the aryl ring of aziridine **1**, contour interval: 25 e/Å^5, blue: negative, red: positive (XDGRAPH[22] representation).

The most eye-catching feature of the deformation density maps in Figure 4 is that the maxima of the deformation density do not correspond to the straight connections between the nuclei. This so called banana bonding phenomenon in highly strained systems has been reported for cyclopropanes and oxiranes in the literature.[1,24] The aziridine three-membered ring differs from the oxirane three-membered ring with respect to the theoretical maps in two ways: First, there is higher loss of density at the oxygen atom than at the nitrogen atom; second, there is a somewhat higher density at the maxima of the C–N bonds in the aziridine than in the C–O bonds of the oxirane. The amount of density between the carbon atoms is about the same. The theoretical and the experimental maps agree well, but the latter reflects the asymmetrical substitution better than the theoretical map. The heightfield representation (Figure 4, d) shows the distribution of the experimental negative Laplacian of the aziridine ring in the bonding regions. The typically saddle shaped bonding region of the homopolar covalent C–C bond with a symmetrical Laplacian distribution and the regions of the heteropolar covalent C–N bonds with unsymmetrical Laplacian distributions can be identified unambiguously. Even the lone pair region of the nitrogen atom is visible behind its core region.

Topological Analysis

According to Bader's theory[3] an atom is the union of a nuclear critical point ((3;-3) critical point) and its associated basin of attracted trajectories of the electron-density gradi-

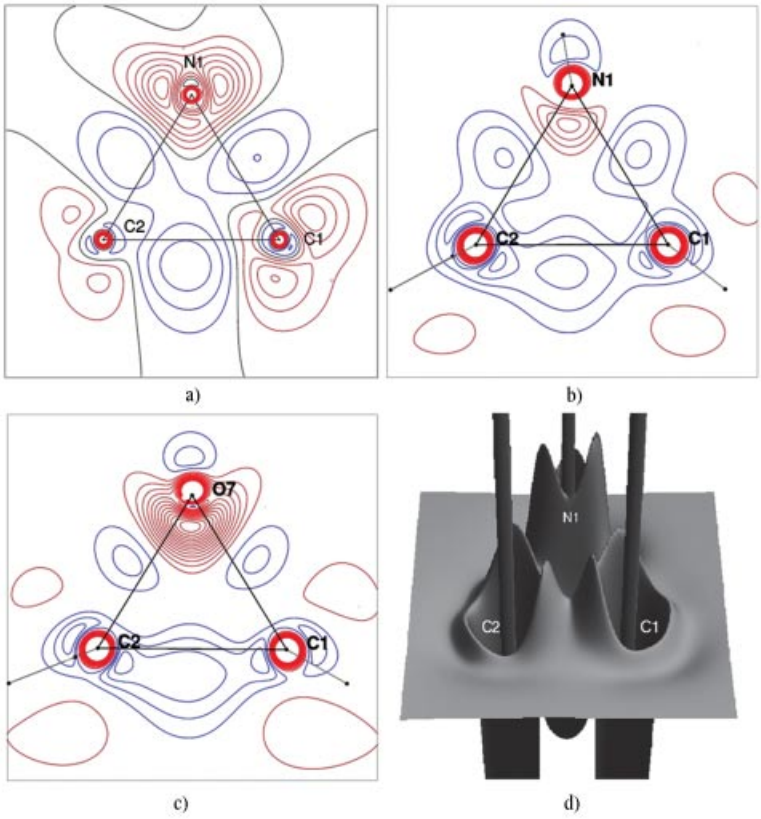

Figure 4. Static deformation density distribution (contour interval: 0.1 e/Å^3, blue: positive, red: negative) of a) aziridine ring of **1** (experiment), b) aziridine ring of **1** (theory), c) oxirane ring of **2** (theory) and the heightfield representation of the experimental negative Laplacian of the aziridine ring of **1** (d)) (XDGRAPH[22] and MOLDEN[23] representations).

 © 2007 Wiley-VCH Verlag GmbH & Co. KGaA, Weinheim

ent vector field $\nabla\rho(r)$ with zero flux surfaces (ZFS) as boundaries, i.e. surfaces that cannot be crossed by any gradient vector except for the bond path. The intersection of a zero-flux surface and a bond path is a bond critical point, a three dimensional saddle point, minimum of the density along the bond path but maximum in two other directions perpendicular to the bond path. A ring critical point is a density minimum in two directions inside the ring's plane being perpendicular to each other and a density maximum perpendicular to the ring's plane. All these properties of Bader's partitioning scheme are visualised in Figure 5 representing the experimental gradient vector fields of the aryl group and the aziridine ring of aziridine **1**.

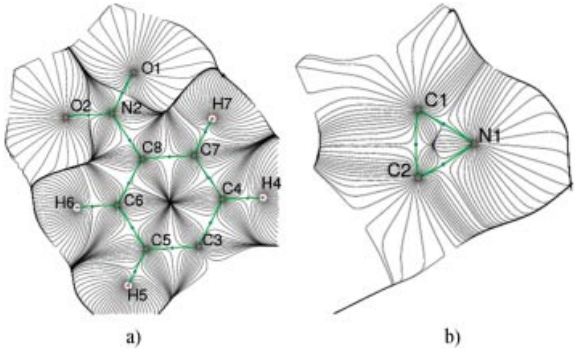

Figure 5. Experimental gradient vector fields of a) the aryl group and b) the aziridine ring. Bond paths and bond critical points are plotted.

Using Bader's theory of atoms in molecules,[3] a topological analysis of the experimentally and theoretically obtained electron-density distribution was performed. Table 3 lists the topological properties of the bond and ring critical points in the reactive regions of compounds **1**–**3**. The theoretical values for the optimised geometry of **1** differ only slightly from the theoretical values for the experimental geometry due to very small changes in the geometry (see above) so that the latter are omitted in the Table.

The values for the experimental density of the N–C bond critical points (bcp) in the aziridine ring are equal to each other with respect to the error margins. The C–C bond of the aziridine contains 0.15 e/Å^3 lower density than the N–C bonds. In the oxirane ring the density loss of the C–C bond is smaller. The qualitative results of the comparison of the theoretical maps in Figure 4 (see above) can be confirmed here: There is slightly higher density at the C–N bcp than at the C–O bcp. The density of the C1–C2 bcp in the olefin compound has the highest value of all C–C bonds as it consists of a double bond. But there seems to be no influence on the densities of the bonds C1–C3, C2–C9 and C2–C11 connecting the substituents to the rings or to the double bond, because they are very similar when comparing all three compounds. The values of the Laplacian for all bcp are negative indicating that all bonds are covalent bonds.

The density of the ring critical point (rcp) of the phenyl ring is about 1.2 e/Å^3 lower than the density of the rcp of the aziridine or oxirane ring because the centre of a smaller ring is much closer to the atoms. The values of the density of the rcp of the aziridine and oxirane ring are almost equal.

The ellipticity is defined as the ratio of the two negative curvatures λ_1 and λ_2 of the Laplace function: $\varepsilon = \lambda_1/\lambda_2 - 1$. It describes the deviation from a cylindrical symmetry of the electron-density distribution at the bcp. For an ideal single bond the value of ε equals 0.0, for a conjugated bond like in benzene ε equals 0.23 and for a double bond like in

Table 3. Density (ρ in e/Å^3), Laplacian ($\nabla^2\rho$ in e/Å^5) and ellipticity (ε) of bond and ring critical points; theoretical values from geometry optimisations.

Bond/ring	Compound	ρ_{exp}	ρ_{theor}	$\nabla^2\rho_{exp}$	$\nabla^2\rho_{theor}$	ε_{exp}	ε_{theor}
N1–C1	aziridine **1**	1.762(14)	1.765	–10.2(1)	–13.0	0.45	0.34
O7–C1	oxirane **2**		1.690		–8.9		0.52
N1–C2	aziridine **1**	1.770(14)	1.766	–8.6(1)	–12.2	0.56	0.34
O7–C2	oxirane **2**		1.733		–10.1		0.50
N1–H1N	aziridine **1**	2.135(10)	2.329	–23.6(1)	–40.1	0.03	0.02
C1–C2	aziridine **1**	1.595(12)	1.557	–9.4(1)	–9.3	0.70	0.49
	oxirane **2**		1.644		–11.5		0.27
	olefin **3**		2.253		–23.2		0.31
C1–C3	aziridine **1**	1.815(14)	1.772	–18.1(1)	–15.7	0.09	0.07
	oxirane **2**		1.779		–15.8		0.08
	olefin **3**		1.836		–16.8		0.08
C1–H1	aziridine **1**	1.791(13)	1.869	–18.4(1)	–22.4	0.05	0.03
	oxirane **2**		1.943		–24.2		0.03
C2–C9	aziridine **1**	1.835(11)	1.771	–16.8(1)	–15.8	0.06	0.06
	oxirane **2**		1.745		–15.2		0.08
	olefin **3**		1.762		–15.7		0.03
C2–C11	aziridine **1**	1.804(12)	1.759	–15.6(1)	–15.2	0.07	0.12
	oxirane **2**		1.719		–14.8		0.10
	olefin **3**		1.767		–15.4		0.13
phenyl ring	aziridine **1**	0.231(19)	0.149	3.1(1)	3.8		
	oxirane **2**		0.149		3.8		
	olefin **3**		0.147		3.8		
three-membered ring	aziridine **1**	1.416(18)	1.379	6.6(1)	4.8		
	oxirane **2**		1.394		7.4		

 © 2007 Wiley-VCH Verlag GmbH & Co. KGaA, Weinheim

ethene ε equals 0.45.[25] In our case ε varies from 0.0 to 0.09 for all single bonds. There are values of ε that are in the region of double bonds: 0.34 to 0.70 for N1/O7–C1, N1/O7–C2 and C1–C2. This finding does not indicate that there are double bonds in the aziridine ring but that there are highly bent single bonds that cause the deviation from a cylindrical symmetry.

Comparing experiment with theory for all bonds of the aziridine compound (cf. electronic Supporting Information) the average deviations are 0.09 e/Å^3 and 5.1 e/Å^5. This is a good agreement between experiment and theory compared to the deviations of 0.08 e/Å^3 and 3.7 e/Å^5 from literature[26] and 0.14(9) e/Å^3 from literature.[27]

The topological analysis of the hydrogen bonds and contacts yielded the values listed in Table 2. Both classical hydrogen bonds (N1A–H1NA···O5A and N1–H1N···N1A) are weak not only regarding the geometrical parameters but also regarding their topology. For strong hydrogen bonds electron-density values of about 0.2 e/Å^3 and more are common.[30] On the other hand, there are several parameters defining a hydrogen bond referring to its topology: There has to be a bond critical point between hydrogen atom and acceptor, the density at the bcp has to be between 0.014 and 0.236 e/Å^3 and the Laplacian at the bcp has to vary between 0.58 and 3.35 e/Å^5.[31] Referring to these criteria all the other C–H···acceptor contacts are weak hydrogen bonds, too. In the literature[5] donor–H···O interactions are referred to as hydrogen bonds even though they are lower in density at the bcp (e.g. 0.03 e/Å^3) and of unfavourable angles (e.g. 108°), but fulfil the conditions given in ref.[31] Thus, one can state that the aziridine compound builds very stable crystals (mechanically and chemically stable) because of its weak but numerous hydrogen bonds stabilising the molecules in the crystal enormously. Figure 6 shows that there are even more interactions than the listed hydrogen bonds. The strongest interaction of 0.085 e/Å^3 on the Hirshfeld surface originates from the contact C11···O3A. The value of this interaction's density on the Hirshfeld surface and at the bcp agree very well (C11···O3A distance: 2.856 Å, symmetry operation: $1-x$, $1-y$, $1-z$, ρ = 0.087(14) e Å^{-3}, $\nabla^2\rho$ = 1.1(1) e Å^{-5}). This example shows that the Hirshfeld surface is not only a useful tool to visualise the molecule's steric demand in the crystal but also to localise all intermolecular interactions with their strength and direction. The hydrogen bonds beginning or ending at the first molecule of the asymmetric unit (Figure 6), namely N1–H1N···N1A (at H1N), C7–H7···O5 (at H7 and O5), C6–H6···O4 (at H6 and O4) and C12A–H12D···N1 (at N1), can be identified on the Hirshfeld surface and density values of about 0.06 e/Å^3 can be read off the scale. This approximated value is in very good agreement with the values of the density at the bcp listed in Table 2 if one considers that a different partitioning scheme to generate Hirshfeld surfaces is used.[28]

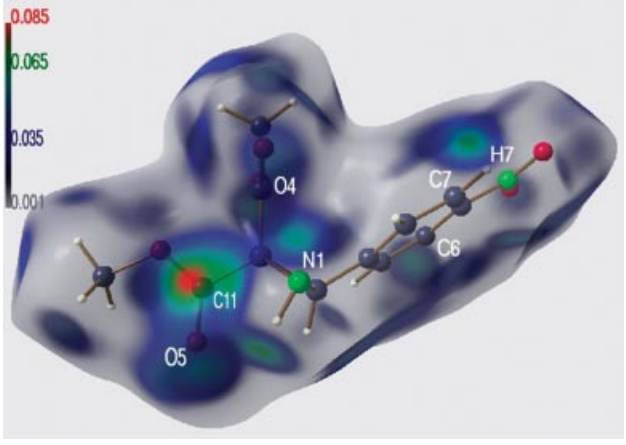

Figure 6. Hirshfeld surface[28] of aziridine **1**, electron density mapped on it, scale in e/Å^3 (MolIso[29] representation, © 2006 Christian B. Hübschle).

Atomic Charges and Volumes

Integrating over the atomic basins yields the atomic volumes and charges. The values from the analysis of the experimentally obtained electron-density distribution of the aziridine ring are summarised in Table 4.

Table 4. Experimental atomic charges (Q_{tot}) and atomic volumes (V_{tot}) of the aziridine ring and environment of aziridine **1**.

Atom	Q_{tot} (e)	V_{tot} [Å^3]
N1	–0.89	14.61
C1	0.10	9.01
C2	0.11	7.39
C3	0.15	8.89
C9	1.67	4.53
C11	1.72	5.05
H1	0.16	5.53
H1N	0.37	3.24

The aziridine ring as a functional group is negatively charged (–0.15 e) due to the large atomic charge of the nitrogen atom. The carbon atoms C1 and C2 that can be attacked from a nucleophile in a ring opening reaction are positively charged as they should be. Thanks to the volume being significantly larger for atom C1, one can assume that an attack is directed towards this carbon atom. Regarding the electrostatic potential (next chapter) this assumption will be confirmed. The carbon atoms C9 and C11 are highly positively charged because they are bound to two oxygen atoms in the ester group. Each of their volumes is about half of the volumes of the carbon atoms C1 and C2 in the aziridine ring that are charged slightly positively. Another striking example for the relationship between atomic volume and charge is the hydrogen atom H1N compared to all the other hydrogen atoms. It carries more than 0.2 e more positive charge than the other hydrogen atoms due to the fact that it is bound to the singly negatively charged nitrogen atom N1 instead of a carbon atom. Consequently, the volume of H1N is about half of the volume of each of the other hydrogen atoms (see electronic Supporting Information).

 © 2007 Wiley-VCH Verlag GmbH & Co. KGaA, Weinheim

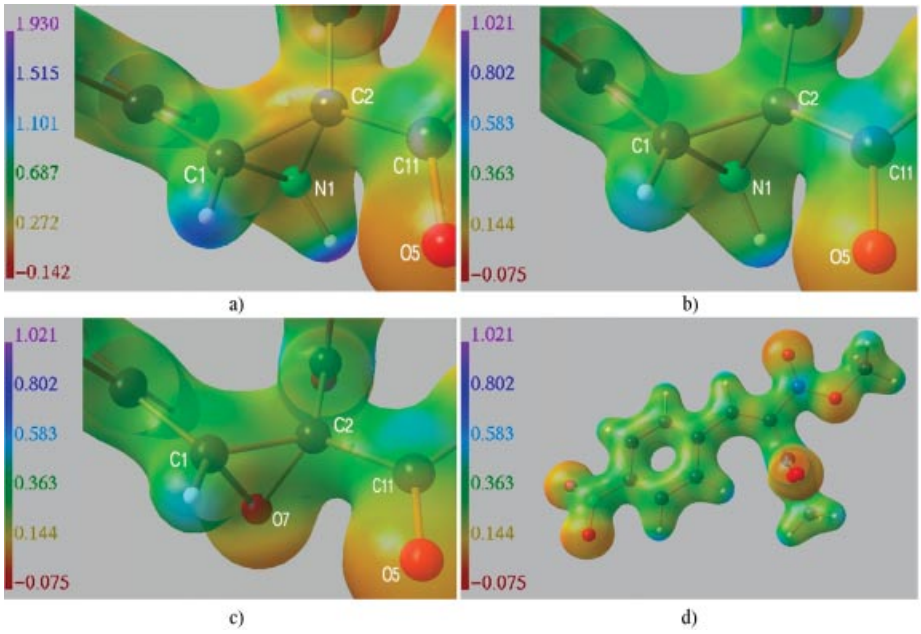

Figure 7. Electrostatic potential mapped on an iso-surface of the density at 0.5 e/Å^3, a) aziridine ring of **1** (experiment), b) aziridine ring of **1** (theory), c) oxirane ring of **2** (theory), d) olefin **3** (theory). Scale in e/Å for experiment, e/a_0 for theory, converted into each other for comparability (MolIso[29] representation).

Electrostatic Potentials

The representation of the electrostatic potential mapped on an iso-surface of the density is very helpful in order to get a deeper insight into the reactivity of the molecules. Figure 7 shows a comparison of the electrostatic potentials of all three compounds. Red coloured regions of the molecules can be regarded as nucleophilic centres while blue regions can be regarded as electrophilic centres. One can see that the distribution of the potential is correlated with the electronegativity of the atoms, as expected. Comparing similar regions of the molecules in theory and experiment it is obvious that charge separation is much more pronounced in the experimental results. This is due to intermolecular interactions in the crystal which can be assumed to be very similar to interactions in biological systems. Thus, the experimental determination of the electron-density distribution is superior to the results of theoretical calculations of isolated molecules in the gas phase if intermolecular interactions are important for the system scrutinised.

Figure 7 allows a close look at the situation in the reactive region of the three-membered rings. The differences between theoretically and experimentally determined electron-density distribution are obvious. In the experimentally derived map (Figure 7, a) the carbon atom C1 is much more positively polarised so that it will be the preferred site for a nucleophilic attack. This finding can be confirmed by chemical experiments (see Scheme 1). Regiospecificity for the attack at C1 can be found. Steric hindrance at C2 also directs the nucleophile to attack at C1. This finding cannot be confirmed by the theoretically derived map (Figure 7, b). No discrimination between the carbon atoms C1 and C2 is possible as it is also not possible for the theoretically derived maps of oxirane and olefin (see parts c,d in Figure 7). The double bond of the olefin compound generates a more negative potential than the conjugated bonds of the phenyl ring do, but the carbon atoms of the double bond are positively polarised. This explains why a nucleophilic addition reaction takes place instead of an electrophilic addition reaction as far as conclusions can be drawn at present from the theoretical results. It is therefore necessary to carry out experimental studies also for oxirane **2** and olefin **3** which are planned as soon as suitable single-crystals are obtained and they will be reported in a forthcoming paper.

Zero Laplacian Iso-Surfaces

The zero Laplacian iso-surface (also called "reactive surface" after Bader[3]) of the aziridine ring (Figure 8) allows an additional insight into the reaction mechanism. Each hole in the iso-surface depicts an electrophilic centre because wherever the value of zero for the Laplacian cannot be reached a reduced valence shell charge concentration is located. So, these holes are the centres where a nucleophilic

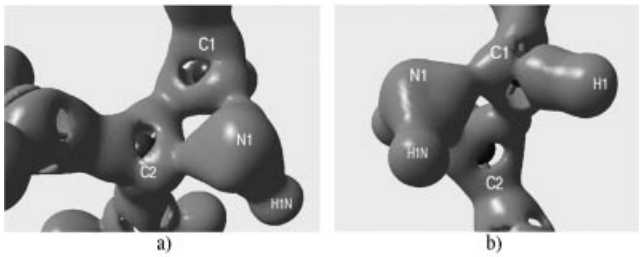

Figure 8. Experimental zero Laplacian iso-surface of aziridine **1**. View from different directions: perspective b) is rotated by about 180° against perspective a). MolIso © 2006 Christian B. Hübschle.

 © 2007 Wiley-VCH Verlag GmbH & Co. KGaA, Weinheim

attack is most probable. Looking at carbon atom C1 from two different directions three holes can be found. None of these holes is preferred regarding their dimensions because the bigger a hole, the greater the electrophilicity. One can assume that the attack will occur from the side of the least steric hindrance, that is from the side of the hydrogen atom H1 instead of the aryl group. Next to the atom H1 there are two holes (Figure 8, b), none of which seems to be the preferred reaction site.

Reactions with Nucleophiles

Aziridine **1** is known to undergo nucleophilic ring opening with acetate under cleavage of the C1–C2 bond of the aziridine ring after acylation with acetic acid anhydride leading to the open-chain product **4a** (Scheme 1).[32] This reaction, which may proceed through the azomethine ylide **1a**, also occurs with propionic acid anhydride leading to the corresponding product **4b** (Scheme 1). In both cases, the nucleophile attacks exclusively at C1 of the aziridine ring. In order to examine if such ring opening reactions also take place without preceeding activation by *N*-acylation, **1** was treated with benzyl mercaptan (Scheme 1). The product **5** obtained hereby also results from C1–C2 bond cleavage with attack of the nucleophilic thiol at C1. No product from attack at C2 could be detected. These results are in a good agreement with the properties of the compound derived from the experimental charge-density determination.

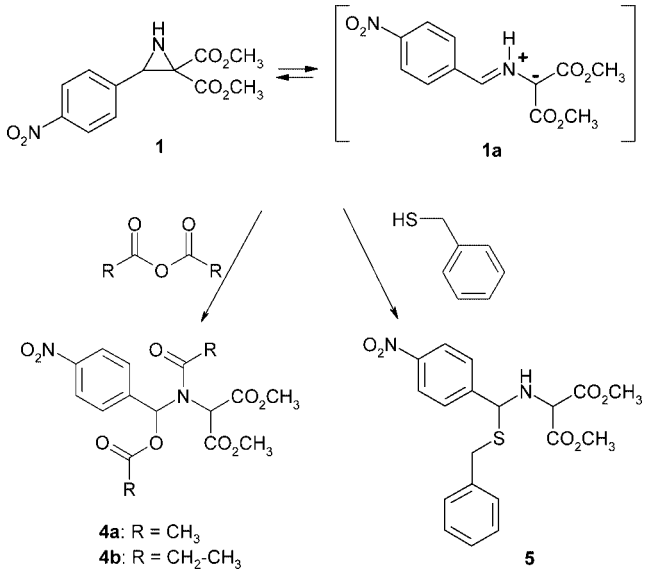

Scheme 1. Reactions of aziridine **1** with nucleophiles. In both cases (reaction with oxygen and sulfur nucleophile) the ring-opened product results from attack at C1 of the aziridine ring.

Conclusions

Experimental electron-density determination by means of ultra-high resolution X-ray diffraction at low temperature is a hitherto rarely exploited tool for the development, optimisation, and analysis of biologically active molecules. We applied this method to dimethyl 3-(4-nitrophenyl)aziridine-2,2-dicarboxylate (**1**), which, together with the corresponding epoxide **2** and the acceptor-substituted olefin **3**, serves as model compound for irreversible cysteine and aspartic protease inhibitors consisting of an electrophilic "war head". The detailed geometrical properties, bonding situations, hydrogen bonding properties, topological properties, atomic charges, and the electrostatic potential of aziridine **1** are determined. With these detailed information it is possible to predict the positions and types of intermolecular non-covalent interactions, as well as the reactive centres of the molecule concerning covalent reactions. A comparison with model reactions with oxygen and sulfur nucleophiles revealed that aziridine **1** reacts according to its determined electronic properties: Attack of the nucleophiles exclusively takes place at C1 which is the more positively polarised carbon atom of the three-membered ring. A comparison of the theoretically and experimentally obtained charge density shows that the experimentally derived properties are much better suited to explain the chemical reactivity of the scrutinised compound. The charge separation is much more pronounced in the experimental results due to intermolecular interactions between the molecules in the crystal. These interactions are generally based on the same forces as complex formation between a biologically active ligand and its macromolecular target. Thus, the experimental electron-density determination is a valid tool to get access to the structural and electronic properties of biologically active molecules, and can be used to understand their non-covalent and covalent modes of action. Therefore experimental studies for oxirane **2** and olefin **3** are planned as soon as suitable single-crystals are obtained.

Experimental Section and Computational Details

Syntheses and Crystallisation: The compounds were synthesised as follows (Scheme 2): olefin **3** was obtained by Knoevenagel condensation of malonate with *p*-nitro benzaldehyde. Epoxidation of **3** with hypochlorite yielded epoxide **2**, and reaction of **3** with diphenylsulfimide led to aziridine **1**.[32]

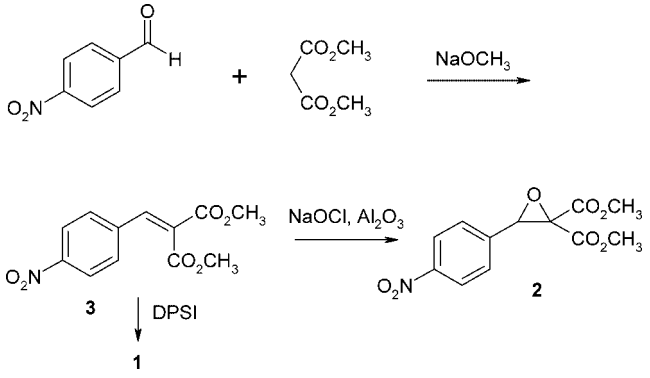

Scheme 2. Synthesis of electrophilic building blocks: acceptor-substituted olefin **3**, epoxide **2**, aziridine **1**.

Compounds **1**–**3** were recrystallised from dichloromethane/methanol. Originally, in no case the crystal quality was sufficient for

 © 2007 Wiley-VCH Verlag GmbH & Co. KGaA, Weinheim

single-crystal diffraction experiments because all compounds tend to form poor diffracting, twinned crystals to a very high degree. After several recrystallisation attempts only from aziridine **1** an appropriate red shining single-crystal with dimensions of $0.45 \times 0.25 \times 0.15\ mm^3$ could be obtained which was suited for high-resolution X-ray diffraction experiments.

X-ray Data Collection: X-ray synchrotron measurements of the single-crystal were performed at the beamline D3 of storage ring DORIS III at HASYLAB/DESY in Hamburg which is equipped with a Huber four circle diffractometer and a MarCCD 165 area detector. A wavelength of 0.56 Å for the primary radiation was chosen. The temperature was maintained at 9 K during the measurement by using an open helium gas flow cooling device (*Helijet, oxford diffraction*). Although several geometric restrictions at the beamline and a triclinic crystal system (space group $P\bar{1}$) existed, 163095 reflections could be measured to a resolution of $(\sin\theta)/\lambda = 1.02\ Å^{-1}$ with a completeness of data of 83.9%.

CCDC-628198 contains the supplementary crystallographic data for this paper. These data can be obtained free of charge from The Cambridge Crystallographic Data Centre via www.ccdc.cam.ac.uk/data_request/cif.

Data Reduction and Refinement: The frames were integrated and corrected with the programme XDS.[33] For scaling and merging the programme XSCALE belonging to the XDS suite was used. The phase problem was solved using the programme SHELXS[34] and yielded all atom positions of the two independent molecules of the asymmetric unit. Conventional spherical refinement was carried out by the programme SHELXL[34], $R(F) = 4.08\%$, to establish the starting positional and displacement parameters (anisotropic for non-hydrogen atoms, isotropic for hydrogen atoms) for the aspherical refinement steps. For aspherical refinement the Hansen–Coppens multipole formalism,[35] implemented in the XD programme package,[36] was used. The chemically most reasonable density model including local symmetries and chemical constraints was applied. For the two crystallographically independent molecules, the multipole model of the second molecule was constrained to that of the first one (see also electronic Supporting Information). That was considered justified from the molecular geometries which were very comparable for both molecules after spherical refinement. C–H and N–H distances were fixed to average values obtained from neutron diffraction analyses.[37] All non-hydrogen atoms were treated up to the hexadecapole level of expansion, while a bond-directed dipole was introduced for all hydrogen atoms. The expansion-contraction parameter κ was refined independently for all non-constrained atoms. The final values of κ did not differ from the starting values of 1.0 by more than 7%. The refinement yielded an aspherical density model with $R(F) = 2.71\%$. For analysing the obtained electron-density distribution the programmes XDPROP and TOPXD of the XD programme package[36] were used.

Quantumchemical Calculations: Single-point ab initio calculations for aziridine **1** at the experimental geometry and optimisations for compounds **1**–**3** were performed using the GAUSSIAN 03 programme package.[38] The density functional B3LYP was combined with the basis set 6-311++G(d,p) that is sufficient for small organic molecules.[39] The theoretically obtained electron-density distribution was analysed using the programme MORPHY98.[40]

Supporting Information (see also the footnote on the first page of this article): Detailed crystallographic data, a description of the refinement strategy, the densities (ρ in e/Å^3), Laplacians ($\nabla^2\rho$ in e/Å^5) and ellipticities (ε) of bond and ring critical points, and the theoretical values from geometry optimisations; the experimental atomic charges (Q_{tot}) and atomic volumes (V_{tot}) of the aziridine ring and environment, and a description of the syntheses and analytical data of compounds **1**, **2**, **3**, **4b**, **5**.

Acknowledgments

Financial support by Deutsche Forschungsgemeinschaft (DFG) is gratefully acknowledged.

[1] T. S. Koritsánszky, P. Coppens, *Chem. Rev.* **2001**, *101*, 1583–1627.
[2] P. Coppens, *Angew. Chem.* **2005**, *117*, 6970–6972.
[3] R. F. W. Bader, *Atoms in Molecules – A Quantum Theory*, Clarendon Press, Oxford, **1995**.
[4] G. Naray-Szabo, *J. Mol. Graphics* **1989**, *7*, 76–81.
[5] R. Flaig, T. Koritsánszky, R. Soyka, L. Häming, P. Luger, *Angew. Chem. Int. Ed.* **2001**, *40*, 355–359.
[6] D. E. Hibbs, C. J. Austin-Woods, J. A. Platts, J. Overgaard, P. Turner, *Chem. Eur. J.* **2003**, *9*, 1075–1083.
[7] N. E. Ghermani, A. Spasojevic-de Bire, N. Bouhmaida, S. Ouharzoune, J. Bouligand, A. Layre, R. Gref, P. Couvreur, *Pharm. Res.* **2004**, *21*, 598–607.
[8] A. Wagner, R. Flaig, B. Dittrich, H. Schmidt, T. Koritsánszky, P. Luger, *Chem. Eur. J.* **2004**, *10*, 2977–2982.
[9] a) J. C. Powers, J. L. Asgian, O. D. Ekici, K. E. James, *Chem. Rev.* **2002**, *102*, 4639–4750; b) H.-H. Otto, T. Schirmeister, *Chem. Rev.* **1999**, *97*, 133–172.
[10] B. M. Dunn, *Chem. Rev.* **2002**, *102*, 4431–4458.
[11] a) R. Vicik, M. Busemann, C. Gelhaus, N. Stiefl, W. Schmitz, F. Schulz, M. Mladenovic, B. Engels, M. Leippe, K. Baumann, T. Schirmeister, *ChemMedChem.* **2006**, *1*, 1126–1141; b) R. Vicik, H. Helten, T. Schirmeister, B. Engels, *ChemMedChem.* **2006**, *1*, 1021–1028.
[12] T. Schirmeister, A. Klockow, *Mini-Rev. Med. Chem.* **2003**, *3*, 585–596.
[13] a) E. Martina, N. Stiefl, B. Degel, F. Schulz, A. Breuning, M. Schiller, R. Vicik, K. Baumann, J. Ziebuhr, T. Schirmeister, *Bioorg. Med. Chem. Lett.* **2005**, *15*, 5365–5369; b) S. H. Verhelst, M. Bogyo, *ChemBioChem* **2005**, *6*, 824–827.
[14] S. Ro, S. G. Baeck, B. Lee, J. H. Ok, *J. Pept. Res.* **1999**, *54*, 242–248.
[15] a) R. Vicik, M. Busemann, K. Baumann, T. Schirmeister, *Curr. Top. Med. Chem.* **2006**, *6*, 331–353; b) M. S. Lall, R. P. Jain, J. C. Vederas, *Curr. Top. Med. Chem.* **2004**, *4*, 1239–1253.
[16] U. Kaeppler, N. Stiefl, M. Schiller, R. Vicik, A. Breuning, W. Schmitz, D. Rupprecht, C. Schmuck, K. Baumann, J. Ziebuhr, T. Schirmeister, *J. Med. Chem.* **2005**, *48*, 6832–6842.
[17] M. N. Burnett, C. K. Johnson, ORTEP-III, *Oak Ridge Thermal Ellipsoid Plot Program for Crystal Structure Illustrations*, Oak Ridge National Laboratory Report ORNL-6895, Oak Ridge, Tennessee, USA, **1996**; implemented in PLATON: A. L. Spek, *Acta Crystallogr., Sect. A* **1990**, *46*, C-34.
[18] N. W. Mitzel, J. Riede, C. Kiener, *Angew. Chem.* **1997**, *109*, 2299–2300; *Angew. Chem. Int. Ed. Engl.* **1997**, *36*, 2215–2216.
[19] E. Espinosa, E. Molins, C. Lecomte, *Chem. Phys. Lett.* **1998**, *285*, 170–173.
[20] E. Keller, SCHAKAL-99, *A Fortran Program for the Graphical Representation of Molecular and Solid-State Structure Models*, Albert-Ludwigs-Universität Freiburg, **1999**.
[21] a) J. Solà, A. Riera, X. Verdaguer, M. A. Maestro, *J. Am. Chem. Soc.* **2005**, *127*, 13629–13633; b) J. P. Glusker, *Acta Crystallogr., Sect. D* **1995**, *51*, 418–427; c) P. M. Takahara, C. A. Frederick, S. J. Lippard, *J. Am. Chem. Soc.* **1996**, *118*, 12309–12321.
[22] *XDGRAPH*, implemented in XD suite of programmes[36].
[23] MOLDEN (version 4.4), in: G. Schaftenaar, J. H. Noordik, *J. Comput. Aided Mol. Des.* **2000**, *14*, 123–134.
[24] a) P. Luger, M. Messerschmidt, S. Scheins, A. Wagner, *Acta Crystallogr., Sect. A* **2004**, *60*, 390–396; b) C. L. Klein, E. D. Stevens, *Acta Crystallogr., Sect. B* **1988**, *44*, 50–55.

 © 2007 Wiley-VCH Verlag GmbH & Co. KGaA, Weinheim

[25] R. F. W. Bader, T. S. Slee, D. Cremer, E. Kraka, *J. Am. Chem. Soc.* **1983**, *105*, 5061–5068.
[26] L. Chęcińska, S. Mebs, C. B. Hübschle, D. Förster, W. Morgenroth, P. Luger, *Org. Biomol. Chem.* **2006**, *4*, 3242–3251.
[27] E. Rödel, M. Messerschmidt, B. Dittrich, P. Luger, *Org. Biomol. Chem.* **2006**, *4*, 475–481.
[28] a) F. L. Hirshfeld, *Theor. Chim. Acta* **1977**, *44*, 129; b) M. A. Spackman, P. G. Byrom, *Chem. Phys. Lett.* **1997**, *267*, 215–220.
[29] C. B. Hübschle, MolIso, in: C. B. Hübschle, P. Luger, *J. Appl. Crystallogr.* **2006**, *39*, 901–904.
[30] C. Flensburg, S. Larsen, R. F. Stewart, *J. Phys. Chem.* **1995**, *99*, 10130–10141.
[31] a) U. Koch, P. L. A. Popelier, *J. Phys. Chem.* **1995**, *99*, 9747; b) P. L. A. Popelier, *J. Phys. Chem. A* **1998**, *102*, 1873.
[32] T. Schirmeister, *Liebigs Ann./Recueil* **1997**, 1895–1899.
[33] XDS (version 12/2004) in: a) W. Kabsch, *J. Appl. Crystallogr.* **1988**, *21*, 916–924; b) W. Kabsch, *J. Appl. Crystallogr.* **1993**, *26*, 795–800.
[34] a) G. M. Sheldrick, SHELXS-97, *Program for Crystal Structure Solution*, **1997**, University of Göttingen, Germany; b) SHELXL-97, *Program for Refinement of Crystal Structures*, **1997**, University of Göttingen, Germany.
[35] N. K. Hansen, P. Coppens, *Acta Crystallogr., Sect. A* **1978**, *34*, 909–921.
[36] T. Koritsánszky, T. Richter, P. Macchi, A. Volkov, C. Gatti, S. Howard, P. R. Mallinson, L. Farrugia, Z. W. Su, N. K. Hansen, XD, *A Computer Program Package for Multipole Refinement and Analysis of Electron Densities from Diffraction Data*, Tech. rep., Freie Universität Berlin, **2003**.
[37] F. H. Allen, O. Kennard, D. G. Watson, L. Brammer, A. G. Orpen, R. Taylor in *International Tables for Crystallography*, vol. C (Ed.: A. J. C. Wilson), Kluwer Academic Publishers, Dordrecht, Boston, London, **1992**, chapter 9.5, pp. 685–706.
[38] *GAUSSIAN 03*, Revision B.04, M. J. Frisch, G. W. Trucks, H. B. Schlegel, G. E. Scuseria, M. A. Robb, J. R. Cheeseman, J. A. Montgomery Jr, T. Vreven, K. N. Kudin, J. C. Burant, J. M. Millam, S. S. Iyengar, J. Tomasi, V. Barone, B. Mennucci, M. Cossi, G. Scalmani, N. Rega, G. A. Petersson, H. Nakatsuji, M. Hada, M. Ehara, K. Toyota, R. Fukuda, J. Hasegawa, M. Ishida, T. Nakajima, Y. Honda, O. Kitao, H. Nakai, M. Klene, X. Li, J. E. Knox, H. P. Hratchian, J. B. Cross, C. Adamo, J. Jaramillo, R. Gomperts, R. E. Stratmann, O. Yazyev, A. J. Austin, R. Cammi, C. Pomelli, J. W. Ochterski, P. Y. Ayala, K. Morokuma, G. A. Voth, P. Salvador, J. J. Dannenberg, V. G. Zakrzewski, S. Dapprich, A. D. Daniels, M. C. Strain, O. Farkas, D. K. Malick, A. D. Rabuck, K. Raghavachari, J. B. Foresman, J. V. Ortiz, Q. Cui, A. G. Baboul, S. Clifford, J. Cioslowski, B. B. Stefanov, G. Liu, A. Liashenko, P. Piskorz, I. Komaromi, R. L. Martin, D. J. Fox, T. Keith, M. A. Al-Laham, C. Y. Peng, A. Nanayakkara, M. Challacombe, P. M. W. Gill, B. Johnson, W. Chen, M. W. Wong, C. Gonzalez, and J. A. Pople, Gaussian, Inc., Pittsburgh, PA, **2003**.
[39] a) B. Dittrich, C. B. Hübschle, M. Messerschmidt, R. Kalinowski, D. Girnt, P. Luger, *Acta Crystallogr., Sect. A* **2005**, *61*, 314–320; b) M. P. Andersson, P. Uvdal, *J. Phys. Chem. A* **2005**, *109*, 2937–2941.
[40] P. L. A. Popelier, R. G. A. Bone, MORPHY-98, *A Topological Analysis Program*, University of Manchester, **1998**.

Received: December 12, 2006
Published Online: March 30, 2007

 © 2007 Wiley-VCH Verlag GmbH & Co. KGaA, Weinheim